Heliyon 9 (2023) e18021

Contents lists available at ScienceDirect

Heliyon

journal homepage: www.cell.com/heliyon

Immediate placement of extra-short implants in refined scapula tip microvascular free flaps: In house virtual planning and surgical technique – Proof of concept☆

Drago Jelovac[a,*,1], Milutin Micic[b,1], Sanela Hajdarevic[a], Cedomir Kuzmanovic[a], Branislav Cukic[c], Branislav Stefanovic[d], Ksenija Zelic[b,e], E.A. Bonfante[f], Rolf Ewers[g], Milan Petrovic[a]

[a] Clinic for Maxillofacial Surgery, School of Dental Medicine, University of Belgrade, Dr Subotica 4, 1100, Belgrade, Serbia
[b] Faculty of Medicine, Center of Bone Biology, University of Belgrade, Dr Subotica 4, 1100, Belgrade, Serbia
[c] Oral B Cukic, Novi Sad, Serbia
[d] Dental Stefanovic, Belgrade, Serbia
[e] School of Dental Medicine, University of Belgrade, Dr Subotica 4, 1100, Belgrade, Serbia
[f] Department of Prosthodontics and Periodontology, University of São Paulo – Bauru School of Dentistry, Bauru, SP, Brazil
[g] University Hospital for Cranio Maxillofacial and Oral Surgery, Medical University of Vienna, Waehringer Guertel 18 - 20, 1090, Vienna, Austria

A R T I C L E I N F O

Keywords:
Scapula tip flap
Microvascular flap
Medical 3D models
Extra short implants
Osteosarcoma
In-house 3D printing
Haptic
Simultaneous implant placement

A B S T R A C T

Scapula tip flaps have been introduced in the literature as an ideal surgical treatment option for large defects in the horizontal plane of the maxilla. This article aims to present a unique step by step protocol for a near total maxillectomy with a pterygoid bone resection and consecutive microvascular reconstruction with a harvested scapula tip flap. The protocol includes immediate placement of extra-short implants in donor bone with the aid of Virtual Surgical Planning (VSP), and an in-house 3D printing of medical 3D models and surgical guides. So far, there has been no presented surgical technique combining immediate implant placement in the scapula region with simultaneous microvascular repair. This technique allows: tumour resection; flap harvesting; extra-short implant placements and reconstruction to be performed in one simultaneous procedure. The technique is presented with illustrations, VSP (presented on videos), radiographs, and surgical findings. We discovered that this refinement of the scapula tip surgery has enabled reconstructive procedures to be performed at the same time as implant placements, providing expedited functional and aesthetic outcomes in selected cases. Moreover, modification of the surgical technique could enhance the competence of the oropharyngeal edge. In conclusion, this new surgical protocol utilizing VSP, 3D models and simultaneous extra-short implant placement provides indispensable advantages for such a complicated surgical procedures, while significantly shortening the duration of surgery.

☆ This study has been supported by SERBIAN ASSOCIATION FOR THE RECONSTRUCTIVE MICROSURGERY OF THE HEAD AND NECK, Ministry of Education, Science and Technological development Grant No. 7750038, and the International transplant study group.

* Corresponding author.
E-mail address: jbdrago@gmail.com (D. Jelovac).

[1] Drago Jelovac and Milutin Micic contributed to this report equally.

https://doi.org/10.1016/j.heliyon.2023.e18021
Received 1 March 2023; Received in revised form 24 June 2023; Accepted 5 July 2023
Available online 7 July 2023

1. Introduction

The free scapula flap technique has been introduced in head and neck surgeries as a reliable transplantation method for various defects in this region [1–4]. These flaps offer high versatility for reconstructions in the maxillofacial region, and the procedure is considered safe with respect to morbidity and complications in both the donor and recipient sites [5].

Prior literature has confirmed that the length and volume harvested in this procedure is safe, owing to the angular branch (AB) of the thoracodorsal artery (TDA), which nourishes the scapula tip. The average distance between the scapula tip and the entry of AB is 4.86 cm (mean) $\pm$ 0.75 cm [6]. Studies have shown that the length of bone nourished by the AB can range from approximately 6 cm–14 cm [4,7], which is considered sufficient for this procedure.

Although scapula tip free flaps meet the criteria needed for the reconstruction of horizontal maxillary defects, many challenges remain. Namely, the final goal – complete recovery of the stomatognathic system including prosthetic reconstruction of occlusion – is not always achieved. Nowadays, the majority of patients who have undergone maxillary microvascular bone repair suffer from an extensive or permanent lack of occlusion, even though the goal of dental reconstruction is to have a prosthesis with permanent aesthetics and function. This is due to the thin plane of the scapula, which limits the bone volume available for implant placement. For this purpose, standard-length implants ($\geq$10 mm–13 mm) are too long [8,9]. Even if the edge of the scapula tip is thicker, bone volume is often still insufficient. As a result, the technique of using the scapula as a source of autologous grafts, followed by implant placement, has not been widely adopted.

To address the issue of the scapula tip having limited bone volume, this manuscript proposes the utilization of extra-short ($\leq$6 mm) implants. These implants have demonstrated a 97.2% survival rate when they were placed in severely atrophic arches and used to support full-arch reconstructions [10]. Leveraging the properties of the extra-short implants, which allows them to be successfully placed in atrophic arches, we present here a surgical technique that enables the immediate extra-oral placement of these implants within the scapula flap, thereby significantly expediting the process of occlusal reconstruction.

The use of 3D printing for in-house production of anatomical models; virtual surgical planning (VSP); and surgical guides have been shown to decrease surgical time and improve the accuracy of reconstructions in complex cases [11–14]. Furthermore, the use of VSP and 3D printed anatomical models facilitate the positioning of implants within the scapula bone.

The extra-oral placement of implants in the scapula bone, although challenging, yields invaluable benefits for the patient. The extra-oral placement of implants enables the simultaneous execution of dental implant placement and scapula tip free flap reconstruction for horizontal maxillary defects – making one-stage surgeries possible for this type of defect.

To the best of our knowledge, there has been no published record of primary implant placement using short (>6 mm to < 10 mm) or

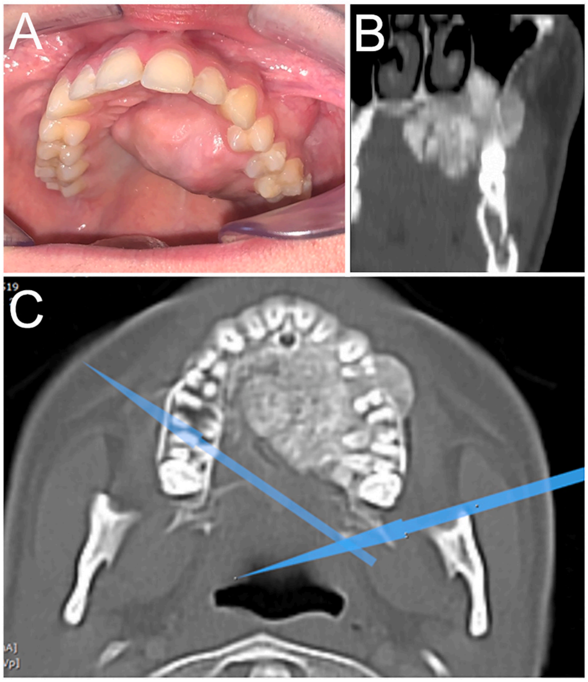

Fig. 1. PREOPERATIVE FINDINGS A- 21-year-old patient, clinical preoperative image of the osteosarcoma of the maxilla. B) Coronal view C) Preoperative CT findings (Preoperative CT findings tumour of the alveolar ridge of maxilla and hard palate, with mixed components, dimensions-38 $\times$ 45 $\times$ 48mm. Blue arrows show posterior resection plane. Calcifications and oedema of the surrounding structures went through the alveolar ridge at the left side into maxillary sinus and contralateral hard palate. (For interpretation of the references to colour in this figure legend, the reader is referred to the Web version of this article.)

extra-short (≤6 mm) [8] implants, in a one-stage procedure, in conjunction with a microvascular scapula tip flap. Furthermore, no reported case existing in the literature describing a singular surgical technique involving simultaneous dental implant placement in scapula donor bone, as a reconstructive procedure following tumour ablation. This is the first report that presents, in detail, a refined surgical technique for harvesting a free scapula tip flap and simultaneously placing extra-short dental implants in the donor scapula bone during ablative surgery. This procedure incorporates the use of 3D medical models and surgical guides to enhance precision and accuracy.

1.1. Case presentation

The male patient was referred to our clinic in the Department of Maxillofaial Surgery, University of Belgrade, for a swelling in the maxillary region. The swelling was not accompanied by any pain or bleeding. His biopsy revealed a high-grade osteosarcoma of the maxilla (Fig. 1A). The extent of the tumour was confirmed using computerized tomography (CT) (Fig. 1B and C) and magnetic resonance imaging (MRI).

A multi-disciplinary team of clinicians decided that the patient should receive neoadjuvant chemotherapy (CHT). Then, when CHT successfully stabilized the disease without significant response (SD) or progression, the surgical phase of his treatment was planned. The patient gave his informed and written consent for this treatment, as well as consent for the publication of the images in this article. The study has been approved by the Ethics Committee of the School of Dental Medicine, Univesity of Belgrade No 36/30.

1.2. Virtual surgical planning and printing of medical 3D models and surgical guides

The most important aspects for the surgery design were performed by means of Virtual Surgical Planning using appropriate software. The patient underwent radiological scanning, during which the recipient region was scanned using a Scanora 3D CBCT scanner (Soredex, Tuusula, Finland) and the donor region was scanned using the SOMATOM Sensation 16 MSCT system (Siemens, Germany). The Digital Imaging and Communication in Medicine (DICOM) files obtained from scanning were imported into 3D Slicer software version 4.10 (Brigham and Women's Hospital, Inc., Boston, MA, USA), where the scans were segmented, separated according to region of interest, and transformed into 3D model files [15]. The 3D models of donor and recipient regions were imported into 3D Studio Max software (Autodesk, Inc., San Rafael, CA, US), in which the models were cleared of double edges and inner voids, then used for VSP and for designing appropriate surgical guides. The printable 3D files of the scapula, maxilla, and surgical guides were then exported and printed using the 3D printing technique of Fused Deposition Modelling (FDM). All models were printed with polylactic acid (PLA) (Shenzhen Creality 3D Technology Co, Ltd, Shenzhen, China), and sterilized in an enclosed chamber using a pair of UV, 8 W, 254 nm wavelength, germicidal light lamps (Sankyo Denki Co Ltd, Japan), at 10 cm distance for 1 h [16,17].

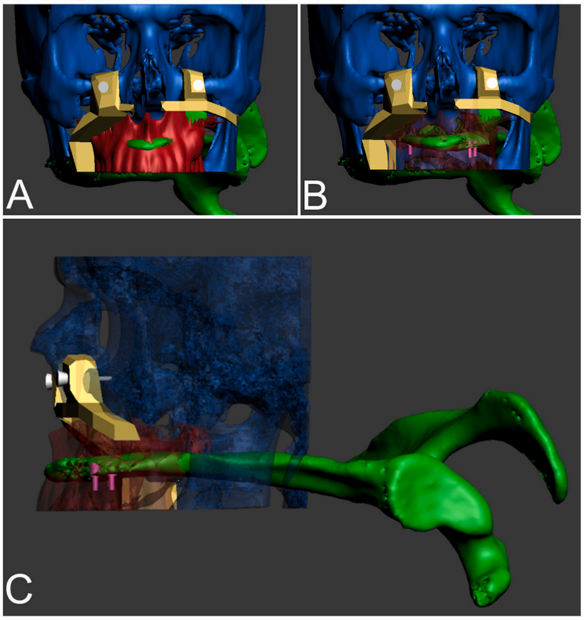

Fig. 2. VIRTUAL PLANNING OF MAXILLARY RECONSTRUCTION: A) Frontal perspective; Patient scull, guides for maxillectomy, guide positioning pins, resection part of the maxilla and scapula labelled respectively with blue, yellow, white, red and green colour. Superimposition of the scapula over the non-jet resected maxilla B) The planned scapula transplant including three implants (labelled with violet colour) superimposed over the non-jet resected transparent maxilla. The predicted position of three implants labelled with violet colour. C) left lateral perspective of maxillary reconstruction elements, with all models transparent, except right scapula model (green). (For interpretation of the references to colour in this figure legend, the reader is referred to the Web version of this article.)

After the VSP, our team used the 3D printed models to design a precise maxillectomy and a donor site flap with adequate shape and volume, such that ideal positioning of the flap in the recipient site could be achieved (Fig. 2).

In our specific case, the extent and localization of the tumour required a subtotal bilateral maxillectomy. The defect was classified as Class III according to Okay [18]. The defect was near total in the horizontal direction of the maxillary plane; while the vertical extent of the maxillectomy at the right and left side were, respectively, low and high Le Fort I osteotomies. The patient's only tooth – the second molar – and the tuberosity region of the right maxilla, were preserved in the surgical plan.

After the virtually performed maxillectomy, the VSP indicated that the scapula tip could reach the maxillary defect and that ideal positioning of the scapula – in the center of the maxillary bone – could be achieved, considering the relative positions of the nasal floor; the anterior nasal spine; the remaining right maxillary tuberosity; and the zygomatic bone on the left side. The planning revealed a gap in the upper part of the scapula's left lateral border, i.e. the left side of the neo maxilla. Consequently, we decided to fill this gap with a 1-cm non-vascularized graft in the form of a bone chip. The bone chip was obtained from the superior part of the scapula, which will be described later. The planning and virtual surgery are presented in Video 1.

The position of the implants was planned virtually and further labelled within the scapula flap with the aid of the scapula tip surgical guide. We planned to insert extra-short 4.0 × 5.0 mm implants (Bicon LLC, Boston, Massachusetts, United States).

After detailed 3D measuring of the scapula thickness, the medial and lateral margin of the scapula revealed 6.7 mm and 7.3–8.1 mm of available bone, respectively, in the area for implant placement. (Fig. 3).

1.3. The surgery

1.3.1. Patient preparation and maxillectomy

Resection lines around the tumour were determined by considering clinical findings, radiographs, and VSP (Figs. 1 and 2). We decided to use the scapula instead of the fibula because of the following reasons: 1) Anatomical characteristics of the defect and their better matching with scapula tip flap; 2) A scapula flap does not require osteotomies; 3) The subscapularis muscle is thought to have better epithelialization than fibula skin island [19,20]; 4) A portion of scapula flaps had very thin bone that ideally matched the horizontal palatine process of the maxilla: 5) Longer pedicle; 6) To provide an additional muscle cuff for two layer oronasal and oral maxillary closures; 7) There was enough bone to place extra short implants. The patient was placed in the supine position, allowing surgeons to assess the operative field in the region of the head and neck.

After general anaesthesia was induced, a tracheostomy was performed. Bilateral Weber Ferguson incisions was performed to expose the entire maxilla. After precise and adequate exposure of the maxilla, 3D custom guides were used for the maxillectomy according to the VSP (Figs. 2 and 4). Hemostasis was achieved, and the defect was packed with gauze. Recipient vessels on the left side of the neck, including the facial and lingual arteries and the thyro-lingual veins, were harvested.

1.4. Surgical technique of scapula tip rising

The donor sites were chosen according to the localization of the defect, and the side of predicted anastomosis of harvested vessels. Our preoperative radiological density assessment showed significantly higher Hounsfield Units (HU) numbers, as well as slightly better

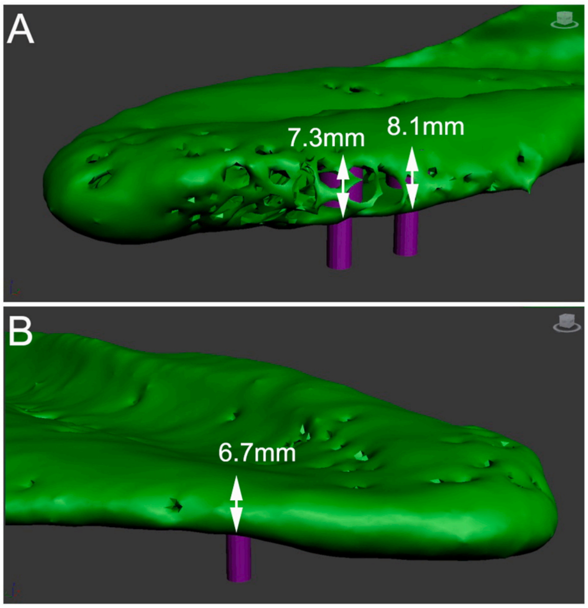

Fig. 3. MEASUREMENTS OF AREA FOR IMPLANT PLACEMENT. A) lateral border of the right scapula tip B) Medial border of the right scapula tip.

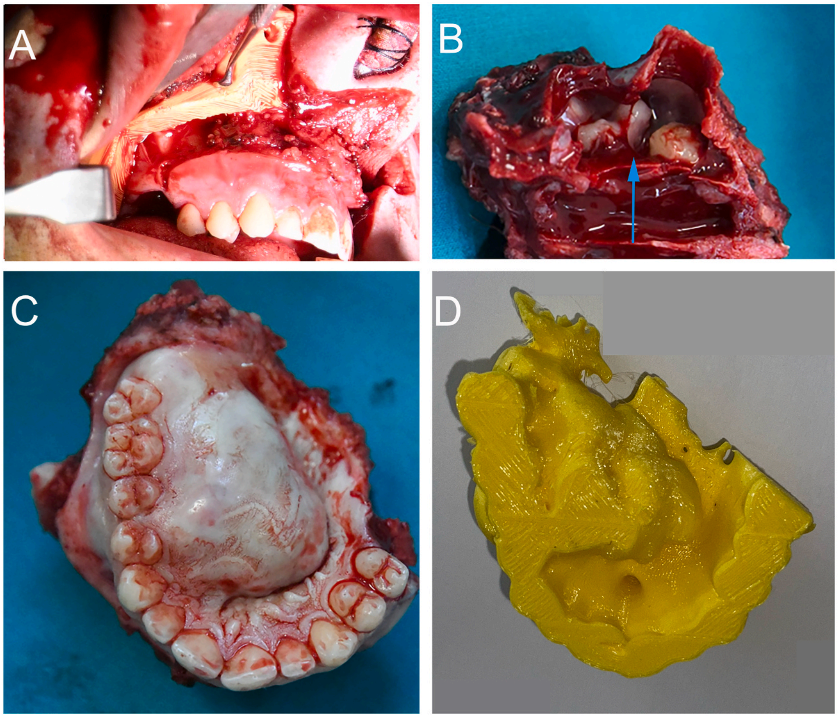

Fig. 4. PLANNING AND SURGERY A) Surgical guide (yellow colour) for right side maxillectomy in place B) Blue arrow shows penetration of the osteosarcoma through the floor of maxillary sinus et the left side of maxilla C) Surgical specimen D) biomodel of resected maxilla (same perspective as surgical specimen confirming accuracy of guided resection). (For interpretation of the references to colour in this figure legend, the reader is referred to the Web version of this article.)

medial and lateral bone margin thickness, for the right scapula compared to the left. Therefore, we selected the right scapula tip as the donor site.

We prefer having a haptic experience before operating on the scapula (Fig. 5). The term "haptic feeling" refers to the tactile sense and touch sensation we can experience on the 3D printed scapula prior to surgery. This haptic experience allows us to better predict the 3D position, orientation, geometry, and potential collisions related to the targeted scapula during the operation.

The patient was placed in a lateral decubitus position for harvesting of the free flap.

A lazy S incision was performed from the posterior axillary fold towards the angle of the scapula. The thoracodorsal (TD) artery was then traced from its origin towards its angular branches. All muscles were sectioned from the lateral border of the scapula in order to access the latissimus dorsi muscle, which had to be retracted down to expose the serratus anterior and teres major muscles, as well as the TD artery and its branches which are usually ligated [4]. Our defect-oriented approach required harvesting a certain volume of muscle to reduce the chances of a postoperative oronasal or oral-maxillary fistula. Therefore, it was important to predict the adequate muscle volume.

Fig. 5. 3D model of the scapula allowed us to have haptic feeling before we operated on the scapula.

The next step involved identifying the osteotomy line of the scapula according to the previously designed surgical guide (Fig. 6). A gap of 5.0 mm between the guide and the scapula was intentionally left for the muscle cuff within the printed guide.

After the scapular bone was exposed, inferior and superior bone cuts were made in it (Fig. 7). We named these cuts "gaining of the muscle cuff for oronasal lining" (Fig. 7). After the subscapularis muscle was exposed, the scapula we required was approached from the medial side. The subscapularis fascia at the site was harvested within the muscle to provide an adequate intraoral lining. We intended the subscapularis muscle on the ventral surface of the scapula to replace the palatal mucosa and become the neo palate. The ventral surface of the scapula – the subscapularis muscle – was positioned toward the oral cavity; and the dorsal surface – the infraspinatus muscle – faced upward toward the nasal cavity. After the pedicle was traced, the harvested scapula was confirmed with the surgical guide (Fig. 6).

One centimeter of the scapula's superior portion was removed (the grey zone of Fig. 7B). This "1 cm osteotomy approach" provides two benefits. Firstly, it yields wider cuffs in the subscapularis and infraspinatus muscles, enabling easier closure with the rest of the soft palate. Second, it yields bone chips, which can be used to fill some asymmetrical defects. This unique modification of the established surgical technique provides an improved oronasal lining with two muscle layers (the suprascapularis and the infraspinatus in Fig. 7J) providing closure between the oral and nasal cavities.

1.4.1. Implant insertion

The implants were inserted into the bone prior to vessel ligation, which seemed to be the only possible option. We inserted three extra-short 4.0 × 5.0 mm implants (Bicon, Bicon LLC, Boston, MA, USA) directly into the ventral surface of the scapula under the subscapularis muscle. Fig. 7 highlights all the important surgical steps required in order to prepare the scapula for implant insertion. First, the subscapularis muscle was retracted from the posterior and lateral aspects of the scapula's ventral surface, along the lateral border of the scapula (Fig. 7D–H). The muscles should be minimally elevated to provide just enough room for implant insertions, as preservation of nourishment for the entire flap was essential. Meticulous and minimal periosteal elevation was also required. After gentle periosteal elevation, the scapular bone should bleed, indicating an uncompromised blood supply. We strongly advise treating the pedicle with care, by protecting it from hazards or stretching during implant insertion. The entire procedure should be performed while the pedicle is loosened up to its origin, to prevent compromising the microcirculation.

The inserted dental implants were secured with sinus lift abutments – small metal parts that prevent the implants from intruding further into the scapula bone. After implant insertions were completed, meticulous stitches were placed on the muscle – now the neo periosteum – in order to protect the implants (Fig. 7H).

1.4.2. Reconstruction of the recipient site

Following implant placement, the donor site was closed, and the defect was then reconstructed with the scapula tip flap. The scapula bone was secured in the defect using plates and screws. In the lateral and anterior aspects of the defect, the cuff of the infraspinatus muscle was stitched to the remaining buccal mucosa. In the posterior aspect of the defect, the cuffs of the infraspinatus and subscapularis muscles were stitched to the nasal mucosa of the soft palate, providing two layers of closure between the oral cavity and nose (Fig. 7J). This is made possible by the previously described "1 cm osteotomy approach", which provided wider cuffs in the subscapularis and infraspinatus muscles, enabling an easier closure with the rest of the soft palate. The improved oronasal lining, with a two-muscle-layer closure between the oral and nasal cavities utilizing the suprascapularis and infraspinatus muscles, is depicted in Fig. 7J. Our osteotomy approach also provided bone chips that serve as non-vascularized grafts, which we used to reconstruct the gap that remained on the left side of the neo maxilla. Anastomoses were performed with recipient vessels of the facial artery and branches of the thyro-linguofacial vein (Carl Zeiss Jena Microscope, ZEISS OPM 241-F manufactured in 1983).

Postoperative radiographs and clinical images revealed that the neo maxilla had been ideally positioned in the patient (Figs. 8–10).

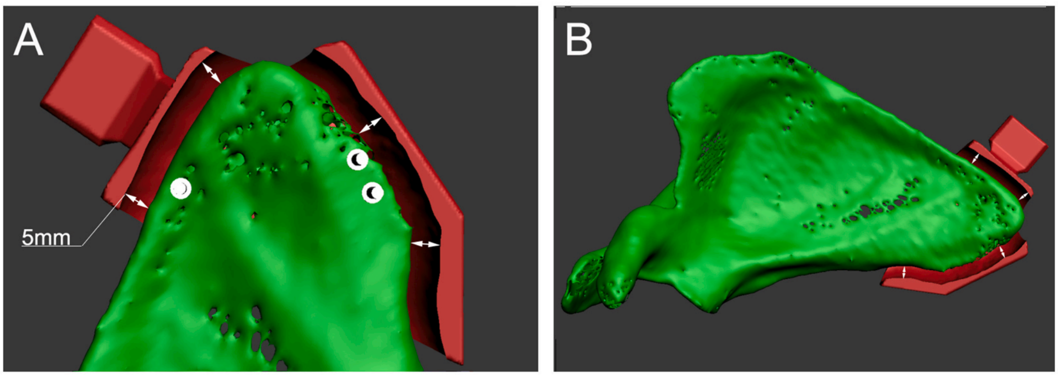

Fig. 6. SCAPULA RESECTION VIRTUAL PLANNING: A) scapula (green) with the resection guide (transparent red), dental implants (pink) positioned B) presents the same elements (scapula tip guide labelled with violet colour) from the same perspective with a gap of 5 mm for soft tissue planned around scapula (green). (For interpretation of the references to colour in this figure legend, the reader is referred to the Web version of this article.)

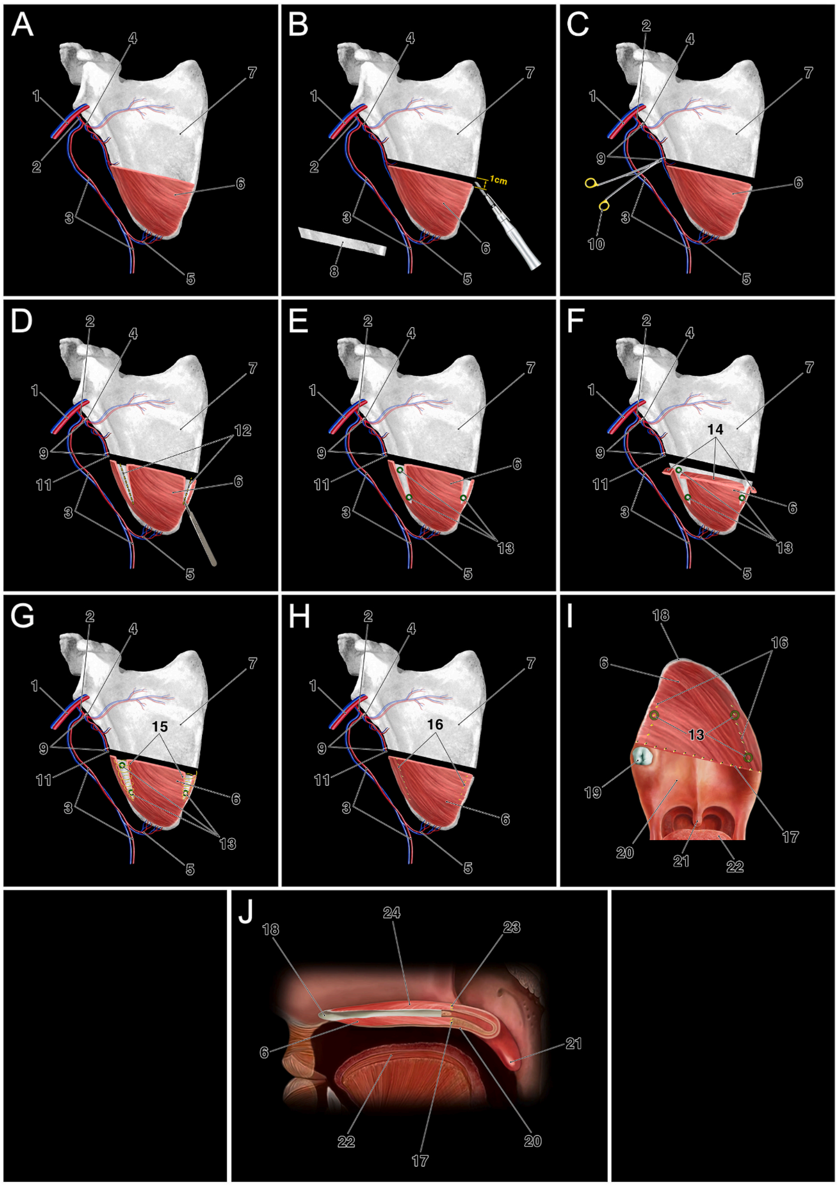

Fig. 7. STEP BY STEP EXPLANATION OF THE TECHNICAL PROCEDURE (A–J) (labelled numbers: (1-26): A- Ventral surface scapula anatomy.
B- "1 cm osteotomy approach"
C- Ligation of the branches of circumflex scapula vessels.
D- Incision over the lateral border in the posterior segment of the flap – elevation of the subscapularis muscle.
E— Exposed bone around the predicted position for implant placement.
F- subscapularis muscle cuff.
G- Stitching of subscapularis muscle and neo periost over the implants.
H- Stitched wound over the implants.
I- Inferior view of the neo maxilla in the oral cavity showed.
J- Double muscle layer closure between the oral cavity and nose.
Labelled Numbers 1. Axillar artery and vein; 2. Subscapular artery and vein; 3. Thoracodorsal artery; 4. A. circumflex scapulae; 5. Angular branch; 6 Subscapularis muscle; 7. Ventral surface of the scapula; 8. 1 cm width osteotomy piece of the scapula achieved with superior and inferior cut of the bone; 9) ligation of periosteal and cutaneous branches of circumflex scapular artery and veins; 10. ligation forceps; 11 ligated periosteal branches; 12. Incision over the lateral border in the posterior segment of the flap through subscapularis muscle; 13. Predicted position of the implants; 14. Cuff of the subscapularis muscle; 15. Suture of subscapularis muscle and neo periost over the implants; 16. Sutured incisions over the implants; 17. Suture line between the posterior border of the flap and soft palate ("oropharyngeal lining"); 18. Tip of the scapula; 19. Remaining second molar in the right tuberosity; 22. Soft palate; 23. Tongue base; 24. Nasal lining (suture of the infraspinatus muscle with remaining nasal layer); 25. Infraspinatus muscle; 26. Uvula.

The clinical image shown in Fig. 9 shows very good horizontal alignment of the neomaxilla in all three directions, with an adequate lip nose angle; optimal anterior-posterior positioning; and ideal occlusion between the remaining maxillary right molar and the lower molars.

1.5. Postoperative clinical and radiological images present a successful surgical approach

Patient showed complication free and fast recovery with regard to both oral cavity function and general health. Although the final assessment will be performed after prosthetic rehabilitation, the patient had no complaints about his nasal breathing and swallowing. His speech was completely intelligible, and will be improved after his dental prosthesis is inserted. Our pathological findings showed complete tumour removal with free surgical margins. However, since the tumour penetrated the sinus floor, poor prognosis is possible.

2. Discussion

The scapula tip free flap technique for reconstructing horizontal maxillary defects has been previously reported [2,3,21,22]. Piazza C. et al. described a similar surgical technique for reconstructing palato-maxillary defects using the angular branch-based tip of the scapula free flap [3]. Kass et al. further highlighted various advantages and challenges associated with the scapula tip free flap [23]. Our article introduces several innovations in the surgical protocol, which enhance the outcome of the procedure. Furthermore, our protocol is significantly enhanced by our utilization of 3D technology and our primary placement of extra-short implants.

There are several advantages of the proposed protocol for simultaneous, extra-oral implant placement: ease of visualization; sustainable bone stabilization with minimal chance of the neo maxilla moving after fixation; shorter ischemia time; one-stage surgery;

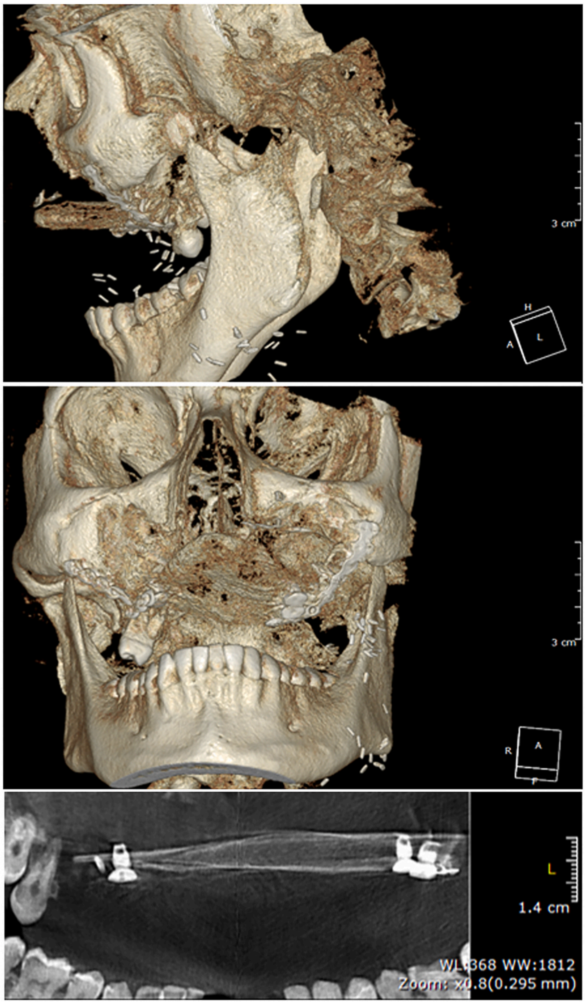

Fig. 8. CBCT radiographic postoperative image.
A) Lateral view, with position of the neomaxilla in 3D view regarding the surrounding structures B) AP projection of the neomaxilla in 3d view C) DVR mode with OPG (ortopantomograph) presented the position of three ultra short implants within the neomaxila

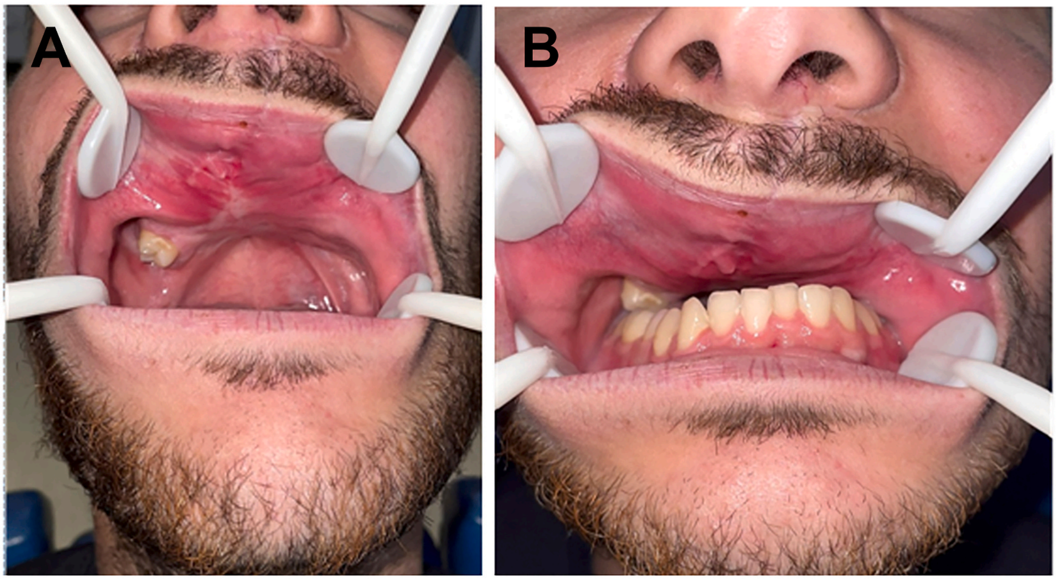

Fig. 9. Postoperative clinical appearance of the patient, 6 MONTHS, intraoral view A) open mouth B) In occlusion.

and avoidance of unnecessary displacements of the reconstructed part, which could happen if the implants were placed intraorally.

From an oncological point of view, simultaneous implant placement is considered a safe and promising approach [24]. A systematic review has shown similar success rates for primary versus secondary placements of standard-length implants in patients receiving vascularized fibula reconstructions. However, it is unknown whether the same is valid for extra-short implants placed in scapula vascularized reconstructions in oncological cases [25]. Therefor, the outcomes of this study would be beneficial for the design of future prospective trials.

In 1988, Ewers demonstrated the importance of double muscle closure of the horizontal maxillary defect, using double mucoperiosteal flaps in connection with a composite calvarian bone graft [26]. In this article we achieved the same goal of double muscle closure, with significant adjustments in our surgical technique. Our findings confirm the importance of two layers of oronasal closure, and our modifications to the surgical protocol has made the oronasal closure more convenient.

A recently published literature review found that VSP and in-house 3D printing led to improved patient outcomes, and thus encouraged these techniques as examples of good practice [15]. So far, the development of in-house 3D printed devices has delivered promising results in the field of oral surgery, suggesting that the technology has reached maturity. The field of clinical applications of VSP is broad and continuously expanding, as it is currently being used from basic clinical applications up to complex surgical challenges. In this article, we present a step-by-step protocol for using VSP combined with immediate extra-oral implant placement in maxillofacial, oncological surgery.

Another surgical technique adjustment presented in this study is the placement of extra-short implants with plateau-root form geometry, where only the outer edges of circumferential fins are in contact with bone. This implant macrogeometry aids in avoiding further bone resorption caused by compression [27,28]. The alternative approach of using tight-fitting threaded implants would have lead to a different osseointegration pathway, where the osteotomies would have undergone extensive interfacial remodelling due to the bone compression and high insertion torque necessary for achieving high primary stability [29,30]. Had we applied this approach, we could have expected significant bone resorption.

Our choice of plateau-roof form implants allowed blood clots to form in the healing chambers between the plateaus, which led to a series of subsequent events fostering a direct and unique osseointegration pathway, and ultimately leading to haversian-like long-term morphology [31]. Considering the challenges of this complex graft procedure, the overall treatment including the use of extra-short implants and macro-geometry may be the key to establishing osseointegration and maintaining peri-implant bone over time, for the following reasons: 1) The use of plateau-root form short implants preserves bone volume and thus promotes the overall nourishment of the grafted scapula; 2) The macro-geometry of the plateau-root form implant leads to direct bone formation in the healing chambers, which likely facilitates osseointegration with the newly donated scapular bone, similar to previously published results of native bone [27,31]; 3) The implant-abutment connection of the plateau-root form implant we used has been previously shown to be hermetic to bacteria, which encourages the establishment and maintenance of a healthy interactions of the implant, abutment, and prosthesis with surrounding tissues [32]. Altogether, since both bone mechanical properties and bone-to-implant contact increase over time around plateau-root form short implants in human non-grafted bone [33,34], it seems reasonable to suggest that similar advantages may be obtained in challenging scapula flap reconstruction scenarios. Future investigations in grafted sites should be performed to confirm these assumptions.

The scapula tip free flap protocol we present, which includes modifications such as the simultaneous placement of extra-short dental implants; VSP; and the in-house 3D printing of bone models and surgical guides, has shown great success. As of the time of

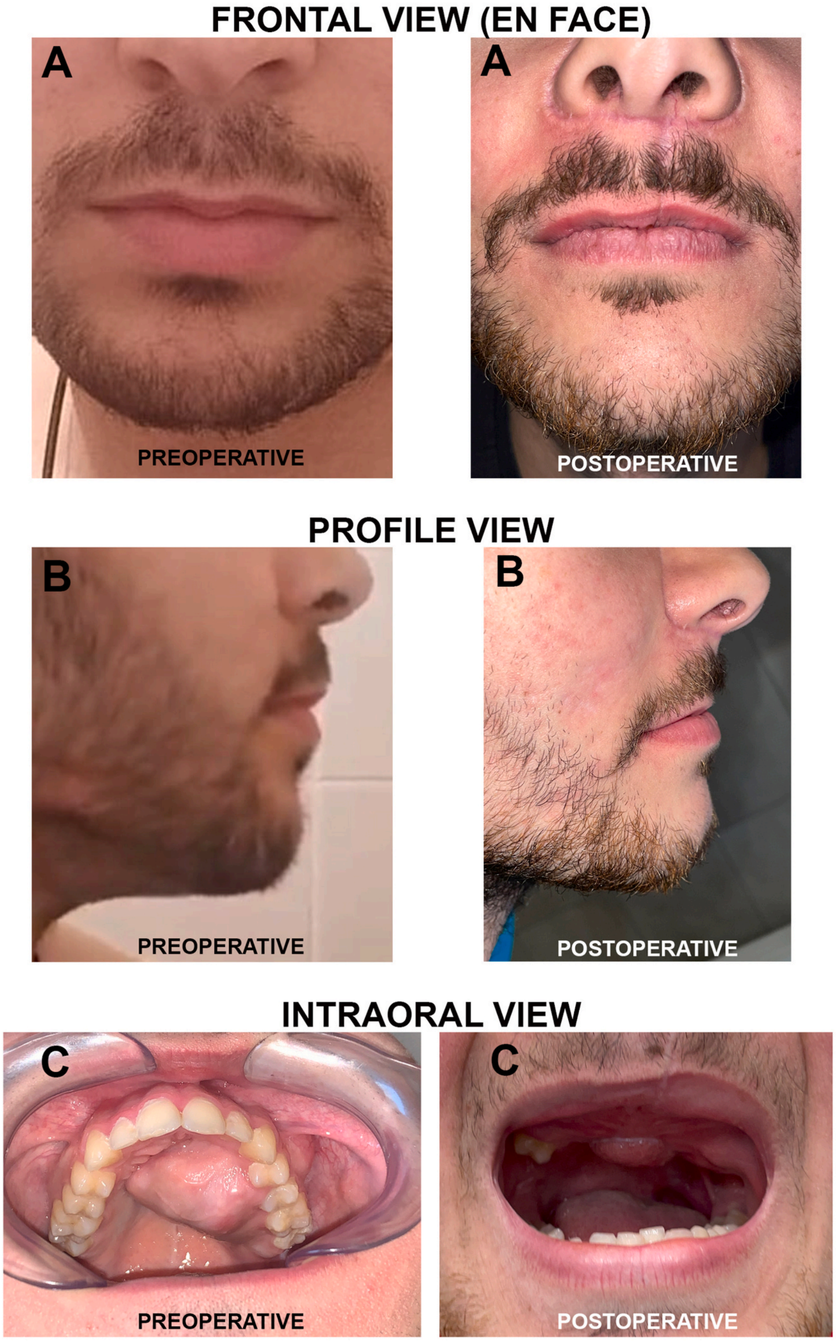

Fig. 10. Preoperative and postoperative photos A) Frontal View B) Profile view C) Intraoral view.

this writing, all implants have been uncovered, and have been confirmed to be fully osseointegrated.

The proposed surgical technique has some limitations. Namely, we did not feel confident with placing dental implants more anteriorly, which would have been ideal for occlusal reconstruction, due to the risk of damaging the flap's nourishment. Thus, the implants were positioned in the posterior part of the neo maxilla. Nonetheless, this scenario is still sufficient for occlusal reconstruction if there are no other possibilities. In scenarios like this one, there exists a proven method for completely reconstructing the maxilla with only three implants, utilizing the CAD/CAM fibre-reinforced hybrid-resin material (TRINIA, Bicon LLC) [35]. Further studies should provide more information regarding the possibility of implant placement in the anterior portion of the scapula tip without compromising the flap's nourishment.

The treatment plan to restore the maxilla involves the use of an overdenture fabricated with a CAD/CAM fiber-reinforced composite

(FRC) framework (TRINIA, Bicon LLC), covered with acrylic resin and acrylic teeth. The cited reference 35 already describes challenging scenarios to restore severely atrophic maxilla with 4, 3 or even 1 short/extra-short implant, as used herein, as well as with FRC supported prostheses. Additionally, recently published clinical research has reported the up to 10 years survival rates of the full-arch mandibular and maxillary arches restored with only 3 short/extra-short implants on FRC frameworks (Fiber-reinforced composite full-arch prosthetic reconstructions supported by three standard, short or extra-short implants: a two-center retrospective study. Cheng YC et al. Clin Oral Investig. 2023 May 4. https://doi.org/10.1007/s00784-023-05035-w. Online ahead of print.). Because this work has shown Kaplan-Meier overall survival rates of 96.5% for implants and of 97.8% for prostheses on native bone we assume that an encouraging prognosis may be expected in this reconstructed maxilla given that similar restorative protocols are planned for this patient.

The treatment plan to restore the maxilla involves the use of an overdenture fabricated with a milled fiber-reinforced composite (FRC) framework (TRINIA, Bicon LLC), covered with acrylic resin and acrylic teeth, as detailed elsewhere [35,36]. Also, recently published clinical research has reported very promising up to 10 years survival rates of full-arch FRC prostheses placed in the mandibular and maxillary arches supported by only 3 short/extra-short implants placed on native bone supported by FRC frameworks [37]. Because this work has shown Kaplan-Meier overall survival rates of 96.5% for implants and of 97.8% for prostheses on native bone we assume that an encouraging prognosis may be expected in this reconstructed maxilla given that similar restorative protocols are planned for this patient.

Although, the prosthetic reconstruction is not presented here, it will be the focus of a future article. Also, prospective follow-ups with larger sample sizes, although a difficult task, are encouraged to report survival rates of the described surgical and restorative protocols.

3. Conclusion

Preoperative virtual surgical planning aided by printed 3D models and guides facilitates the simultaneous placement of extra-short implants during the harvesting of vascular scapular bone, and should greatly assist the treatment of complex maxillectomy cases.

Author contribution statement

Drago Jelovac: Milutin Micic: Rolf Ewers: Conceived and designed the experiments; Performed the experiments; Analyzed and interpreted the data; Contributed reagents, materials, analysis tools or data; Wrote the paper.

Sanela Hajdarevic: Milan Petrovic: Cedomir Kuzmanovic: Conceived and designed the experiments; Performed the experiments; Contributed reagents, materials, analysis tools or data; Wrote the paper.

Branislav Cukic: Branislav Stefanovic: Ksenija Zelic: Analyzed and interpreted the data; Contributed reagents, materials, analysis tools or data; Wrote the paper.

EA Bonfante: Analyzed and interpreted the data; Wrote the paper.

Data availability statement

No data was used for the research described in the article.

Author agreement statement

We the undersigned declare that this manuscript is original, has not been published before and is not currently being considered for publication elsewhere. We confirm that the manuscript has been read and approved by all named authors and that there are no other persons who satisfied the criteria for authorship but are not listed. We further confirm that the order of authors listed in the manuscript has been approved by all of us. We understand that the Corresponding Author is the sole contact for the Editorial process. He/she is responsible for communicating with the other authors about progress, submissions of revisions and final approval of proofs Signed by all authors as follows:

Drago Jelovac, Milutin Micic, Sanela Hajdarevic, Cedomir Kuzmanovic, Branislav Cukic, Branislav Stefanovic, Ksenija Zelic, Estevam Bonfante.

Declaration of competing interest

The authors declare that they have no known competing financial interests or personal relationships that could have appeared to influence the work reported in this paper.

Appendix A. Supplementary data

Supplementary data to this article can be found online at https://doi.org/10.1016/j.heliyon.2023.e18021.

References

[1] V. Uglesic, M. Virag, S. Varga, P. Knezević, A. Milenović, Reconstruction following radical maxillectomy with flaps supplied by the subscapular artery, J. Cranio-Maxillo-Fac. Surg. 28 (3) (2000) 153–160, https://doi.org/10.1054/jcms.2000.0137.

[2] S. Ferrari, A. Ferri, B. Bianchi, Scapular tip free flap in head and neck reconstruction, Curr. Opin. Otolaryngol. Head Neck Surg. 23 (2) (2015) 115–120, https://doi.org/10.1097/MOO.0000000000000137.

[3] C. Piazza, A. Paderno, Bon F. Del, V. Taglietti, A. Grammatica, N. Montalto, P. Nicolai, Palato-maxillary reconstruction by the angular branch-based tip of scapula free flap, Eur. Arch. Oto-Rhino-Laryngol. 274 (2) (2017) 939–945, https://doi.org/10.1007/s00405-016-4266-0.

[4] J.R. Clark, M. Vesely, R. Gilbert, Scapular angle osteo-myogenous flap in post-maxillectomy reconstruction: defect, reconstruction, shoulder function, and harvest technique, Head Neck 30 (1) (2008) 10–20, https://doi.org/10.1002/hed.20649.

[5] M. Lanzer, T. Gander, K. Grätz, C. Rostetter, D. Zweifel, M. Bredell, Scapular free vascularised bone flaps for mandibular reconstruction: are dental implants possible? J. Oral Maxillofac. Res. 6 (3) (2015) e4, https://doi.org/10.5037/jomr.2015.6304.

[6] A. Sahovaler, H. Low, F. Laxague, E.J. Chung, K. Fung, S.D. Mac Neil, A.C. Nichols, J. Yoo, Variations of the thoracodorsal axis: application for scapular tip free flap harvesting, Oral Maxillofac. Surg. 26 (4) (2022) 619–623, https://doi.org/10.1007/s10006-021-01037-8.

[7] S. Seneviratne, C. Duong, G.I. Taylor, The angular branch of the thoracodorsal artery and its blood supply to the inferior angle of the scapula: an anatomical study, Plast. Reconstr. Surg. 104 (1) (1999) 85–88, https://doi.org/10.3390/jcm9082322.

[8] S.S. Al-Johany, M.D. Al Amri, S. Alsaeed, B. Alalola, Dental implant length and diameter: a proposed classification scheme, J. Prosthodont. 26 (3) (2017) 252–260, https://doi.org/10.1111/jopr.12517. Epub 2016 Jul 5.

[9] C.S. Burke, C.S. Roberts, J.A. Nyland, P.G. Radmacher, R.D. Acland, M.J. Voor, Scapular thickness–implications for fracture fixation, J. Shoulder Elbow Surg. 15 (5) (2006) 645–648, https://doi.org/10.1016/j.jse.2005.10.005.

[10] R. Ewers, M. Marincola, P. Perpetuini, A. Morina, E.T. Bergamo, Y.C. Cheng, E.A. Bonfante, Severely atrophic mandibles restored with fiber-reinforced composite prostheses supported by 5.0-mm ultra-short implants present high survival rates up to eight years, J. Oral Maxillofac. Surg. 80 (1) (2022) 81–92.

[11] M.C. Modest, E.J. Moore, K.M. Abel, J.R. Janus, J.R. Sims, D.L. Price, K.D. Olsen, Scapular flap for maxillectomy defect reconstruction and preliminary results using three-dimensional modeling, Laryngoscope 127 (1) (2017) E8–e14, https://doi.org/10.1002/lary.26351.

[12] A. Tel, F. Costa, S. Sembronio, A. Lazzarotto, M. Robiony, All-in-one surgical guide: a new method for cranial vault resection and reconstruction, J. Cranio-Maxillo-Fac. Surg. 46 (6) (2018) 967–973, https://doi.org/10.1016/j.jcms.2018.03.020.

[13] X. Yuan, M. Xuan, W. Tian, J. Long, Application of digital surgical guides in mandibular resection and reconstruction with fibula flaps, Int. J. Oral Maxillofac. Surg. 45 (11) (2016) 1406–1409, https://doi.org/10.1016/j.ijom.2016.06.022.

[14] J.J. Xia, C.V. Phillips, J. Gateno, J.F. Teichgraeber, A.M. Christensen, M.J. Gliddon, J.J. Lemoine, M.A.K. Liebschner, Cost-effectiveness analysis for computer-aided surgical simulation in complex cranio-maxillofacial surgery, J. Oral Maxillofac. Surg. 64 (12) (2006) 1780–1784, https://doi.org/10.1016/j.joms.2005.12.072.

[15] D. Ostaș, O. Almășan, R.R. Ileșan, V. Andrei, F.M. Thieringer, M. Hedeșiu, H. Rotar, Point-of-Care virtual surgical planning and 3D printing in oral and cranio-maxillofacial surgery: a narrative review, J. Clin. Med. 11 (22) (2022) 6625, https://doi.org/10.3390/jcm11226625.

[16] S. Pieralli, B.C. Spies, V. Hromadnik, R. Nicic, F. Beuer, C. Wesemann, How accurate is oral implant installation using surgical guides printed from a degradable and steam-sterilized biopolymer?, 9, J. Clin. Med. 22 (8) (2020) 2322, https://doi.org/10.3390/jcm9082322.

[17] S.R. Godbole, T.M. Dahane, N.A. Patidar, S.V. Nimonkar, Evaluation of the effect of ultraviolet disinfection on dimensional stability of the polyvinyl silioxane impressions. An in-vitro study, J. Clin. Diagn. Res. 8 (9) (2014) ZC73–ZC76, https://doi.org/10.7860/JCDR/2014/8461.4875.

[18] D.J. Okay, E. Genden, D. Buchbinder, M. Urken, Prosthodontic guidelines for surgical reconstruction of the maxilla: a classification system of defects, J. Prosthet. Dent 86 (4) (2001) 352–363, https://doi.org/10.1067/mpr.2001.119524.

[19] S.A. Anain, R.J. Yetman, The fate of intraoral free muscle flaps: is skin necessary? Plast. Reconstr. Surg. 91 (6) (1993) 1027–1031, https://doi.org/10.1097/00006534-199305000-00009.

[20] S. Fan, Y.Y. Wang, D.H. Wu, D.L. Lai, Y.H. Feng, X. Yu, Z.Y. Lin, D.M. Zhang, W.L. Chen, J.Q. Liang, J.S. Li, Intraoral lining with the fibular osteomyofascial flap without a skin paddle during maxillary and mandibular reconstruction, Head Neck 38 (Suppl 1) (2016) E832–E836, https://doi.org/10.1002/hed.24109.

[21] J.S. Brown, R.J. Shaw, Reconstruction of the maxilla and midface: introducing a new classification, Lancet Oncol. 11 (10) (2010) 1001–1008, https://doi.org/10.1016/S1470-2045(10)70113-3.

[22] G. Molteni, L. Gazzini, C. Plotegher, L. Lanaro, A. Fior, D. Marchioni, P.F. Nocini, Reconstruction of complex oromandibular defects in head and neck cancer: role of the chimeric subscapular free flap, J. Craniofac. Surg. 1 (3) (2020) e266–e270, https://doi.org/10.1097/SCS.0000000000006277.

[23] J.I. Kass, E. Prisman, B.A. Miles, Guide design in virtual planning for scapular tip free flap reconstruction, Laryngoscope Investig. Otolaryngol. 3 (3) (2018) 162–168, https://doi.org/10.1002/lio2.162.

[24] M. Knitschke, C. Bäcke, D. Schmermund, S. Böttger, P. Streckbein, H.P. Howaldt, S. Attia, Impact of planning method (conventional versus virtual) on time to therapy initiation and resection margins: a retrospective analysis of 104 immediate jaw reconstructions, Cancers 13 (12) (2021), https://doi.org/10.3390/cancers13123013.

[25] A. Ardisson, P. Senna, R. Granato, E. Bergamo, E. Bonfante, C. Marin, Success rate of mandible implants placed in vascularized fibula bone graft: a systematic review, J. Oral Implantol. 21 (2022), https://doi.org/10.1563/aaid-joi-D-20-00104 (Epub ahead of print).

[26] R. Ewers, Reconstruction of the maxilla with a double musculoperiosteal flap in connection with a composite calvarial bone graft, Plast. Reconstr. Surg. 81 (3) (1988) 431–436, https://doi.org/10.1097/00006534-198803000-00021.

[27] E.A. Bonfante, P.G. Coelho, J.M. Navarro, L.F. Pegoraro, G. Bonfante, V.P. Thompson, N.R. Franc, A. Silva, Reliability and failure modes of implant-supported Y-TZP and MCR three-unit bridges, Clin. Implant Dent. Relat. Res. 12 (3) (2010) 235–243, https://doi.org/10.1111/j.1708-8208.2009.00156.x.

[28] M. Lanzer, T. Gander, K. Grätz, C. Rostetter, D. Zweifel, M. Bredell, Scapular free vascularised bone flaps for mandibular reconstruction: are dental implants possible? J. Oral Maxillofac. Res. 6 (3) (2015) e4, https://doi.org/10.5037/jomr.2015.6304.

[29] F.E. Baires-Campos, R. Jimbo, E.A. Bonfante, M.T. Fonseca-Oliveira, C. Moura, D. Zanetta-Barbosa, P.G. Coelho, Drilling dimension effects in early stages of osseointegration and implant stability in a canine model, 2015, Med. Oral Patol. Oral Cir. Bucal 20 (4) (2015) e471–e479, https://doi.org/10.4317/medoral.20557.

[30] S.A. Gehrke, S. Taschieri, M. Del Fabbro, P.G. Coelho, Positive biomechanical effects of titanium oxide for sandblasting implant surface as an alternative to aluminium oxide, J. Oral Implantol. 41 (5) (2015) 515–522, https://doi.org/10.1563/AAID-JOI-D-13-00019.

[31] E.A. Bonfante, R. Jimbo, L. Witek, N. Tovar, R. Neiva, A. Torroni, P.G. Coelho, Biomaterial and biomechanical considerations to prevent risks in implant therapy, Periodontol. 2000 81 (1) (2019) 139–151, https://doi.org/10.1111/prd.12288.

[32] S. Dibart, M. Warbington, M.F. Su, Z. Skobe, In vitro evaluation of the implant-abutment bacterial seal: the locking taper system, Int. J. Oral Maxillofac. Implants 20 (2005) 732–737.

[33] M. Baldassarri, E. Bonfante, M. Suzuki, C. Marin, R. Granato, N. Tovar, P.G. Coelho, Mechanical properties of human bone surrounding plateau root form implants retrieved after 0.3-24 years of function, J. Biomed. Mater. Res. B Appl. Biomater. 100 (7) (2012) 2015–2021, https://doi.org/10.1002/jbm.b.32786. Epub 2012 Aug 4.

[34] L.F. Gil, M. Suzuki, M.N. Janal, N. Tovar, C. Marin, R. Granato, E.A. Bonfante, R. Jimbo, J.N. Gil, P.G. Coelho, Progressive plateau root form dental implant osseointegration: a human retrieval study, J. Biomed. Mater. Res. B Appl. Biomater. 103 (6) (2015) 1328–1332, https://doi.org/10.1002/jbm.b.33311. Epub 2014 Nov 4.

[35] R. Ewers, M. Marincola, P. Perpetuini, Treating the atrophic maxilla with four, three, or even one ultrashort implant, J. Dent. Maxillofacial. Res. 3 (2) (2021) 43–58, https://doi.org/10.30881/jdsomr.00046.
[36] R. Ewers, E.A. Bonfante, Short® implants and TRINIA® full-arch prostheses for the rehabilitation of the atrophic maxilla, in: M. Rinaldi (Ed.), Implants and Oral Rehabilitation of the Atrophic Maxilla Advanced Techniques and Technologies, Springer, 2023, https://doi.org/10.1007/978-3-031-12755-7 (Chapter 8), pag183-208.
[37] Y.C. Cheng, P. Perpetuini, L. Murcko, M. Hirayama, K. Morgan, M. Marincola, E.A. Bonfante, E.T.P. Bergamo, R. Ewers, Fiber-reinforced composite full-arch prosthetic reconstructions supported by three standard, short or extra-short implants: a two-center retrospective study, Clin Oral Investig. May 4 (2023), https://doi.org/10.1007/s00784-023-05035-w. Epub ahead of print. PMID: 37140762.